

Robust Feature Extraction From Hand Biometric Images Using Orthogonal Moments

Lakshmi Deepika C, Kandaswamy A

Department of Biomedical Engineering, PSG College of Technology, Coimbatore-4

Email: cldeepika@yahoo.com, kandaswamy@yahoo.com

Abstract

Biometric verification has in recent times become a part of several consumer applications. Robust methods are therefore required to accurately represent the biometric images in verification algorithms. Orthogonal moments are invariant shape descriptors that can provide enough discrimination power to objects belonging to different classes. However orthogonal moments extract the global properties of an image rather than local ones. In biometric recognition, both the global and local features are required for accurate matching. It is proposed to overcome this limitation of moments by opting for a global feature extraction from localised regions, where the images are subdivided into blocks and the moments are calculated from each block. In this paper we have computed the matching accuracy for the unsampled and sampled biometric images namely the fingerprint and palmprint and found that it is considerably higher in case of sampled images.

Index Terms: Fingerprint, Palmprint, Biometrics, ROI Extraction, Shape, Legendre Moments, Pseudo Zernike Moments, Bayes Net Classifier

Introduction

Moments are scalar quantities used to characterize a function and to capture its significant features. From a mathematical point of view, moments are ‘projections’ of a function onto a polynomial basis. If the polynomial basis is orthogonal, that is, if the elements satisfy the condition of orthogonality, then the moments are called orthogonal moments. In this paper, continuous orthogonal moments namely the Legendre moments and Pseudo Zernike moments are chosen for fingerprint representation. Orthogonal moments extract the global properties of an image rather than local ones [1]. A global feature condenses the characteristic of an object to be measured into one piece of information and also eliminates a lot of false positives caused by local features alone [2]. But when the relative orientation of certain features

is important for the system, local features are preferred. Therefore, combining gist based features with local image features may lead to better feature descriptors.

There are several approaches to fingerprint recognition in literature where both local and global features are combined to give better accuracy [3] combine the local features namely minutia and the global statistical features from fingerprints and their results show improvements in accuracy [4] combine the local features extracted using Gabor filters and global information extracted using wavelet transform. However this method is proposed only for small databases. Further these methods require two different algorithms to process the images and a suitable fusion is also required to combine the local and global features [5] use the global Fourier descriptors which will also simultaneously local ridge information and ridge frequency. This method gives significantly accurate results at lower computational costs. Similar approaches are also found in palmprint recognition. Orientation maps at different scales can be used to represent the local as well as global information [6] and the experimental results are claimed to be very good. [7] use Gabor filters to extract the local information and then increase the scale of the Gabor filters to infinity as to get the Fourier transform of the image which gives the global descriptors. The results obtained are reported to be significantly better than the methods using either only local or only global features for feature extraction. [8] use Contourlet transforms, an extension of wavelet transforms that use the contour segments and fine details in images to realize the local and global information. Thus the extraction of both the local and global features using the same feature descriptors is suggested in recent literature.

In this paper, it is proposed to extract global as well as local features with orthogonal moments by opting for a global feature extraction from localised regions, where the images are subdivided into blocks and the moments are calculated from each block. The fingerprint images are sampled on a 10 x 10 grid and then the moments are extracted and further classified with a Bayesian Belief Network. The classification accuracy is compared with that obtained by using moments obtained from unsampled images. The rest of the paper is organised as follows: Section 2 describes the pre-processing of the fingerprint images. The next section describes the method of extraction of moments from fingerprint images. Section 4 provides the experimental results which make use of the Bayesian classifiers for classification of the features from unsampled fingerprint images. In Section 5, extraction of moments is performed from fingerprint images sampled over a 10 x 10 grid. Classification is done and the improvement in accuracy is elaborated in the same section. Conclusions are given in the last section.

Pre-Processing of Fingerprint and Palmprint

Fingerprint

There are four different databases in FVC 2002 [9] and we have used the set DB1. It is composed of 800 fingerprint images derived from 100 individuals with eight images per finger. These fingerprint images are enhanced, binarised and segmented. The pre-processing is shown in Figure 1.

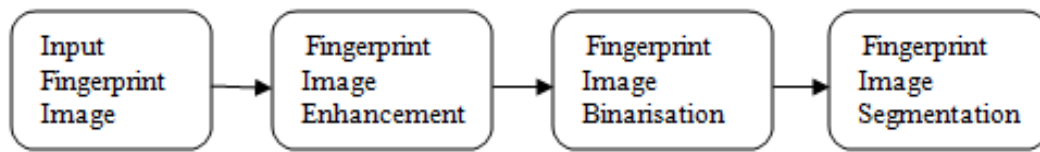


Figure 1: Pre-processing of Fingerprint

A conventional Gaussian filter is used for noise removal and smoothening. A fingerprint's uniqueness is characterised by the ridges which are nothing but sharp discontinuities in the image. These discontinuities are variations in gray levels or the intensities. They are therefore affected when the illumination is not uniform or sufficient. Hence a fingerprint enhancement method adopted should be able to improve the contrast so as to make all details in the image prominent and also for an edge sharpening to make the edge segmentation more efficient. The wavelet-based normalization method [10] was found to be very much suitable for the above requirements. In this method the contrast and edges of the fingerprint images are enhanced simultaneously using the wavelet transform. Wavelet-based image analysis decomposes an image into approximate coefficients and detail coefficients. Contrast enhancement can be done by histogram equalization of the approximation coefficients and meanwhile edge enhancement can be achieved by multiplying the detail coefficients with a scalar (>1). A normalized image is obtained from the modified coefficients by inverse wavelet transform. Using trial and error, db10 1st level wavelet decomposition and 1.5 as the scalar value for multiplying the detail coefficient were fixed. Binarisation of the image is done using an adaptive threshold based binarization method Raghavendra et al [11]. This method involves transformation of the pixel values to 1 in case if the value of the pixel is larger than the mean intensity value of the current block in which the pixel is present, as seen in equation (1).

$$I_{new}(n_1, n_2) = \begin{cases} 1 & \text{if } I_{old}(n_1, n_2) > \text{Local Mean} \\ 0 & \text{otherwise} \end{cases} \quad (1)$$

A two step method is followed to segment the region of interest from the binarized image. The first step involves estimation of the block direction along with direction variety check. The second step involves two morphological operations called 'OPEN' and 'CLOSE'. The operator 'OPEN' expands the image, eliminates the peaks due to background noise and the latter shrinks the images and removes minute cavities.

Palm Print

The palmprint images are taken from the PolyU Palmprint database [12]. The database contains 7752 gray scale images corresponding to 386 users. These images are pre-processed before classification as seen in Figure 2.

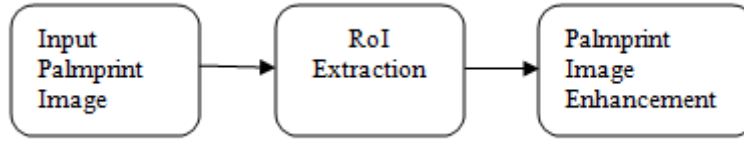


Figure 2: Pre-Processing of Palmprint

Gaussian smoothing is applied to the input image for noise removal. The filtered image is then binarised using an appropriate threshold ‘t’.

$$B(x,y)=1, \text{ if } O(x,y) \geq t \quad (2)$$

$$B(x,y)= 0, \text{ if } O(x,y) < t \quad (3)$$

where, $B(x, y)$ and $O(x, y)$ are the binary image and the original image, respectively. The center of the palm is extracted since it contains the principal lines and wrinkles. Wavelet based normalization is used to enhance the extracted region of the palm [10]

Feature Extraction

Orthogonal moments are moments to an orthogonal or weighted orthogonal-polynomial basis. The continuous orthogonal moments namely Legendre Moments (LM) and Pseudo-Zernike Moments (PZM) are chosen for fingerprint and palmprint representation. If $f(x,y)$ is the intensity function of an image, Legendre moments [13] of order $(m + n)$ are given by (4)

$$\lambda_{mn} = \frac{(2m+1)(2n+1)}{4} \int_{-1}^1 \int_{-1}^1 P_m(x) P_n(y) f(x, y) dx dy \quad (4)$$

where $P_m(x)$ is the m th order Legendre polynomial, $x \in [-1, 1]$ and $m, n = 0, 1, 2, \dots, \infty$. These polynomials form a complete orthogonal basis set over the interval $[-1, 1]$.

The two dimensional Zernike moments [14] of order p with repetition q of an image intensity function $f(r, \theta)$ are defined as

$$Z_{pq} = \frac{p+1}{\pi} \int_0^{2\pi} \int_0^1 V_{pq}(r, \theta) f(r, \theta) r dr d\theta; |r| \leq 1 \quad (5)$$

where Zernike polynomials $V_{pq}(r, \theta)$ are

$$V_{pq}(r, \theta) = R_{pq}(r) e^{-jq\theta}; j = \sqrt{-1} \quad (6)$$

and the real-valued radial polynomial, $R_{pq}(r)$

$$R_{pq}(r) = \sum_{k=0}^{\frac{p-|q|}{2}} (-1)^k \frac{(p-k)!}{k! (\frac{p-|q|}{2} - k)! (\frac{p+|q|}{2} - k)!} r^{p-2k} \quad (7)$$

where $0 \leq |q| \leq p$ and $p - |q|$ is even.

The Legendre moments obtained from all the fingerprint and palmprint images are classified using Bayesian classifiers. When classification is done, the Bayes' classification rule is to allot a test vector ' x ' to class which has the biggest posterior probability $p(w_i/x)$ that is, if $p(w_1/x) > p(w_2/x)$, then the vector is allotted to class w_1 rather than class w_2 . The Baye's Rule states that for any two events A and B , $p(B/A) = p(A/B) \times p(B)$ where $p(A)$ is the probability of ' A ', $p(B)$ is the probability of ' B ', $p(A/B)$ is the probability of ' A ' given that ' B ' has occurred. Using the Bayes formula, $p(w_1/x)$ can be rewritten as $p(x/w_1)p(w_1)$ and $p(w_2/x)$ can be rewritten as $p(x/w_2)p(w_2)$ so that if $p(x/w_1)p(w_1) > p(x/w_2)p(w_2)$, then the vector is allotted to class w_1 rather than class w_2 . Thus the Baye's classification rule minimizes the total probability of misclassification. Errors happen when samples of Class 1 are incorrectly classified to belong to Class 2 and samples of Class 2 are classified to belong to Class 1. A binary classification model which classifies each instance into any one of two given classes gives rise to four possible outcomes: a True Positive (TP), a True Negative (TN), a False Positive (FP) and a False Negative (FN). The Classification Accuracy is given by

$$\text{Accuracy (\%)} = \frac{TP + TN}{TP + FP + TP + FN} \quad (8)$$

Similarly the images represented using pseudo-Zernike moments are classified.

Experimental Results

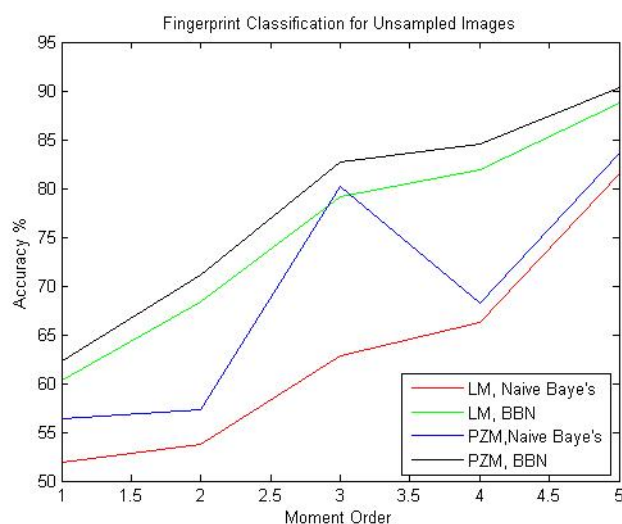
Finger Print

The fingerprint images represented using the Pseudozernike and Legendre moments are classified using two Bayesian classifiers, namely the Naive Bayes' classifier and Bayesian Belief Network. The classifiers are trained with the moments obtained from the fingerprint data set. The classification is done for each order of the two moments separately. In each case, 50% of the data set has been used for training and the remaining 50% is used for testing. The classification results for all moments up to order 5 are shown in Table 1.

Table 1: Classification of orthogonal moments from whole fingerprint images

Moments	Classifier	Performance	Order 1	Order 2	Order 3	Order 4	Order 5
PZM	Naïve Baye's	Accuracy(%)	56.38	57.29	80.2	68.27	83.62
	Naïve Baye's	TP	0.563	0.572	0.802	0.682	0.836
	Naïve Baye's	FP	0.059	0.057	0.020	0.055	0.018
	BBN	Accuracy(%)	62.3	71.1	82.7	84.5	90.3
	BBN	TP	0.623	0.711	0.827	0.845	0.903
	BBN	FP	0.035	0.026	0.017	0.015	0.008
LM	Naïve Baye's	Accuracy(%)	51.85	53.81	62.84	66.24	81.52
	Naïve Baye's	TP	0.518	0.538	0.628	0.662	0.815
	Naïve Baye's	FP	0.064	0.060	0.063	0.057	0.019
	BBN	Accuracy(%)	60.3	68.4	79.2	81.9	88.7
	BBN	TP	0.603	0.684	0.792	0.815	0.887
	BBN	FP	0.039	0.030	0.018	0.016	0.010

It can be seen from Table 1 that the maximum accuracy obtained of 90.3% is obtained at order 5 of Pseudo Zernike moments using the Bayesian Belief Network. A comparison of the accuracy rates of the moments is given in Figure 3.

**Figure 3:** Comparison of Performance of Moments from whole Fingerprint images

The classification accuracy decreases beyond the moment order 5 due to the accumulation of error as the moment order increases. The error present is due to the discretisation error that occurs in situation where the continuous Legendre and pseudo-Zernike moments have to be calculated for discrete images.

Palm Print

The palm print images represented using the Pseudozernike and Legendre moments are classified using the Naive Bayes' classifier and Bayesian Belief Network. The classifiers are trained with the moments obtained from the palm print data set. The classification is done for each order of the two moments separately. In each case, 50% of the data set has been used for training and the remaining 50% is used for testing. The classification results for all moments up to order 5 are shown in Table 2

Table 2: Classification of Moments From Whole Palmprint Images

Moments	Classifier	Performance	Order 1	Order 2	Order 3	Order 4	Order 5
PZM	Naïve Baye's	Accuracy(%)	56.32	64.53	69.52	68.65	79.24
	Naïve Baye's	TP	0.563	0.645	0.695	0.686	0.792
	Naïve Baye's	FP	0.054	0.047	0.040	0.042	0.024
	BBN	Accuracy(%)	63.4	69.7	77.4	85.4	90.1
	BBN	TP	0.634	0.697	0.774	0.854	0.901
	BBN	FP	0.044	0.037	0.025	0.014	0.009
LM	Naïve Baye's	Accuracy(%)	59.27	61.25	69.52	72.82	80.45
	Naïve Baye's	TP	0.592	0.612	0.695	0.728	0.804
	Naïve Baye's	FP	0.057	0.041	0.054	0.030	0.020
	BBN	Accuracy(%)	65.5	74	86.4	88.7	92.5
	BBN	TP	0.655	0.74	0.864	0.887	0.925
	BBN	FP	0.032	0.022	0.015	0.013	0.008

It can be seen from Table 2 that the maximum accuracy of 92.5% is obtained at order 5 of Legendre moments using the Bayesian Belief Network. A comparison of the accuracy rates of the moments is given in Figure 4.

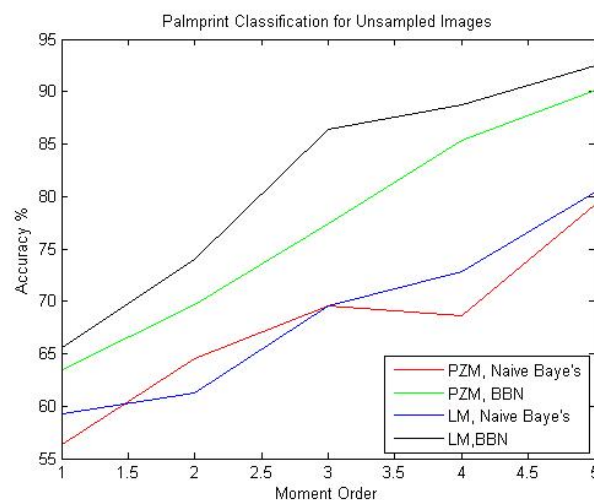


Figure 4: Comparison of Performance of Moments from whole Palmprint images

The classification accuracy decreases beyond the moment order 5 due to the accumulation of error as the moment order increases. The error present is due to the discretisation error that occurs in situation where the continuous Legendre and pseudo-Zernike moments have to be calculated for discrete images.

Extraction of Local and Global Features Using Moments

It is proposed to opt for a global feature extraction from localised regions. There are two approaches to localise an image, namely, sparse and dense approaches. In the 'Sparse' method, the image is decomposed into localised image patch descriptors around interest points or keypoints. In the 'Dense' method, the image is divided into localised image patch descriptors on a regular grid, that is, here the image is 'sampled' over a regular grid [15]. The fingerprint and palmprint images are sampled into $n \times n$ blocks where 'n' is an integer, and then orthogonal moments are extracted from each block. Division into equal sized blocks has the advantage that a good and equal coverage of the entire image is obtained. Since moments are extracted from all the blocks, each block is able to contribute to the detail extracted from the image. However, when the sampling is too dense, the total number of features obtained from all the blocks grows unacceptably large and this will bring down the performance of the system.

Finger Print

The Bayesian Belief Network is used to classify the moments obtained from the sampled fingerprint dataset and results obtained are shown in table 3.

Table 3: Classification of moments from sampled fingerprint images

Mom-ents	Or-der	Perfor-mance	2x2	3x3	4x4	5x5	6x6	7x7	8x8	9x9	110x 10	111x 11	112x 12
PZM	1	Accur-acy(%)	84.2	82.5	74.8	72.1	89.2	90.6	88.1	89.7	91.4	87.2	85.6
		TP	0.842	0.825	0.748	0.721	0.892	0.906	0.881	0.897	0.914	0.872	0.856
		FP	0.014	0.016	0.017	0.019	0.008	0.02	0.012	0.073	0.010	0.012	0.013
	2	Accur-acy(%)	88.2	87.5	85.8	86.8	81.9	83.1	87.2	90.9	94.3	89.4	88.1
		TP	0.882	0.875	0.858	0.868	0.819	0.831	0.872	0.909	0.943	0.894	0.881
		FP	0.011	0.013	0.015	0.014	0.022	0.018	0.0156	0.006	0.0015	0.010	0.014
	3	Accur-acy(%)	89.6	88.7	88.1	88.7	91.2	88.1	94.3	96.7	96.89	92.8	91.6
		TP	0.896	0.887	0.881	0.887	0.912	0.881	0.943	0.967	0.9689	0.928	0.916
		FP	0.008	0.009	0.0094	0.009	0.005	0.009	0.003	0.002	0.002	0.0045	0.005
LM	1	Accur-acy(%)	83.6	81.8	73.7	71.9	88.7	90.2	91.1	89.3	87.6	86.6	85.1
		TP	0.836	0.818	0.737	0.719	0.887	0.902	0.911	0.893	0.876	0.866	0.851
		FP	0.015	0.016	0.018	0.020	0.010	0.008	0.007	0.009	0.012	0.013	0.014
	2	Accur-acy(%)	87.8	87.1	85.2	86.4	81.4	82.6	93.9	90.3	86.7	88.9	87.8
		TP	0.878	0.871	0.852	0.864	0.814	0.826	0.939	0.903	0.867	0.889	0.878
		FP	0.011	0.012	0.014	0.013	0.016	0.015	0.006	0.008	0.013	0.010	0.011
	3	Accur-acy(%)	89.1	88.3	87.8	88.2	90.7	87.6	96.10	96.2	93.8	92.3	89.1
		TP	0.891	0.883	0.878	0.882	0.907	0.876	0.961	0.962	0.938	0.923	0.891
		FP	0.010	0.011	0.012	0.011	0.008	0.012	0.002	0.003	0.006	0.007	0.010

The consistent increase in accuracy at higher moment orders is noticed in table 3 and the accuracy of classification is also seen to vary for each grid size, with the maximum accuracy obtained for a grid size of 10 x 10. For 10 x 10 subimages, Pseudo-zernike moments of order 1 give a classification accuracy of 91.4%, the accuracy is 94.3% for order 2 and the accuracy for order 3 is 96.89%. The maximum accuracy is achieved at moment order 3 with a TP of 0.9689 and FP of 0.002. In case of Legendre moments also, the accuracy of classification is also seen to vary for each grid size, and maximum accuracy is obtained for a grid size of 8 x 8. For 8 x 8 subimages, Legendre moments of order 1 give a classification accuracy of 91.1%, the accuracy is 93.9% for order 2 and the accuracy for order 3 is 96.10%. The maximum accuracy is achieved at moment order 3 with TP of 0.961 and FP of 0.002. Here also it is noted that the classification accuracy of the fingerprint images is higher for their representation using Pseudo Zernike moments.

Palm Print

The Bayesian Belief Network is used to classify the moments obtained from the sampled palm print dataset and the accuracies obtained are shown in table 4

Table 4: Classification of moments from sampled palmprint images

Mom-ents	Or-der	Perfor-mance	2x2	3x3	4x4	5x5	6x6	7x7	8x8	9x9	110x10	111x11	112x12
PZM	1	Accur-acy(%)	84.8	83.1	83.6	82.1	84.3	86.2	88.5	89.4	91.8	90.4	84.8
		TP	0.848	0.831	0.836	0.821	0.843	0.862	0.885	0.894	0.918	0.904	0.848
		FP	0.015	0.016	0.016	0.018	0.015	0.013	0.011	0.010	0.008	0.009	0.015
	2	Accur-acy(%)	87.4	86.2	85.4	87.7	89.4	90.3	91.5	93.1	94.2	93.3	87.4
		TP	0.874	0.862	0.854	0.877	0.894	0.903	0.915	0.931	0.942	0.933	0.874
		FP	0.012	0.013	0.014	0.012	0.010	0.009	0.008	0.007	0.005	0.007	0.012
	3	Accur-acy(%)	89.7	88.5	87.3	89.4	91.6	93.4	94.7	95.8	96.4	95.1	89.7
		TP	0.897	0.885	0.873	0.894	0.916	0.934	0.947	0.958	0.964	0.951	0.897
		FP	0.010	0.011	0.012	0.010	0.008	0.007	0.006	0.005	0.004	0.005	0.010
LM	1	Accur-acy(%)	85.2	83.1	75.4	72.5	90	91	88.4	90.5	92	87.5	85.2
		TP	0.852	0.831	0.754	0.725	0.9	0.91	0.884	0.905	0.92	0.875	0.852
		FP	0.013	0.015	0.016	0.017	0.006	0.01	0.010	0.07	0.009	0.011	0.013
	2	Accur-acy(%)	89.4	88.1	86.5	87.2	82.4	83.5	87.6	91.8	95	90	89.4
		TP	0.894	0.881	0.865	0.872	0.824	0.835	0.876	0.918	0.95	0.9	0.894
		FP	0.012	0.014	0.017	0.016	0.021	0.020	0.016	0.008	0.003	0.011	0.012
	3	Accur-acy(%)	90.1	89.2	88.5	89.4	91.6	88.7	94.7	95.2	97.74	93.3	90.1
		TP	0.901	0.892	0.885	0.894	0.916	0.887	0.947	0.952	0.974	0.933	0.901
		FP	0.007	0.008	0.009	0.007	0.006	0.009	0.004	0.004	0.003	0.005	0.007

It is observed that when the sampling is too dense, the total number of features obtained from all the blocks grows unacceptably large and this will bring down the performance of the system. The experimental results show deterioration in performance when the parameter 'n' exceeds 12. The accuracy of classification is seen to vary for each grid size, and maximum accuracy is obtained for a grid size of 10 x 10. For 10 x 10 subimages, Legendre moments of order 1 give a classification accuracy of 92%, the accuracy is 95% for order 2 and the accuracy for order 3 is 97.74%. The maximum accuracy is achieved at moment order 3 with TP of 0.974 and FP of 0.003.

Conclusion

This paper compares the performance of orthogonal moments for unsampled and sampled fingerprint and palmprint images using Bayesian Belief Network. Experimental results reveal that the Pseudozernike and Legendre moments obtained from sampled fingerprint and palmprint images lead to higher classification accuracy when compared to moments extracted from whole images. Further this high accuracy is obtained at a lower moment order when compared to the moment order at which good accuracy is obtained in whole images. The Pseudozernike moments from the

sampled fingerprint images give a classification accuracy of 96.10% with TP of 0.961 and FP of 0.002 at moment order 3 for a grid size of 8x8 while an accuracy of 90.3% with TP of 0.903 and FP of 0.008 is obtained for whole images at moment order 5. The Legendre moments from the sampled palmprint give a classification accuracy of 97.74% with TP of 0.974 and FP of 0.004 at moment order 3 for a grid size of 10 x 10 while an accuracy of 92.5% with TP of 0.925 and FP of 0.008 is obtained for whole images.

References

- [1] Mukundan, R. and Ramakrishnan, K.R. "Moment Functions in Image Analysis: Theory and Applications", World Scientific Publication Co., Singapore, 1998
- [2] Tuytelaars, T. "Dense Interest Points", Proceedings of the IEEE Conference on Computer Vision and Pattern Recognition, pp. 2281-2288, 2010
- [3] Shi, P., Tian, J., Xie, W.H. and Yang, X. "Fast Fingerprint Matching Based on the Novel Structure Combining the Singular Point with Its Neighborhood Minutiae", Proceedings of CIARP06, pp. 804-813, 2006.
- [4] G Nikam, S., Goel, P., Tapadar, R., and Agarwal, S. "Combining Gabor Local texture pattern and wavelet global features for fingerprint matching", Proceedings of Conference on Computational Intelligence and Multimedia Applications, pp. 409-416, 2008
- [5] Chikkerur, S., Cartwright, N. and Govindaraju, V. "K-plet and CBFS: A graph based fingerprint representation and matching algorithm", Proceedings of the International Conference on Biometrics, 2006.
- [6] Min Ki Kim, "Palmprint Verification using Multi-scale Gradient Orientation Maps", Journal of the Optical Society of Korea, Vol.15, Issue 1, pp. 15-21 (2011)
- [7] Nan Luo, Zhenhua Guo, Gang Wu, Changjiang Song, "Local-global based Palmprint Verification", Proceedings of International Conference on Advanced Computer Control, pp. 543-547, 2011
- [8] Ardabili, E. , Maghooli, K., Fatemizadeh, E. "Contourlet Features extraction and Adaboost Classification for palmprint verification", Journal of American Science, Vol. 7,
- [9] <http://bias.csr.unibo.it/fvc2002/>
- [10] S. Du and R. Ward, Wavelet-based illumination normalization for face recognition, Proc. of the IEEE International Conference on Image Processing, September 2005
- [11] Raghavendra, R., Rao, A. and Hemantha Kumar, G. "A Novel Three Stage Process for Palmprint Verification", Proceedings of the International Conference on Advances in Computing, Control and Telecommunication Technologies, pg 88-92, 2009.
- [12] <http://www.comp.polyu.edu.hk/~biometrics/>

- [13] Mukundan, R. and Ramakrishnan, K.R. "Moment Functions in Image Analysis: Theory and Applications", World Scientific Publication Co., Singapore, 1998.
- [14] Liao, S.X. and Pawlak, M. "On the accuracy of Zernike moments for image analysis", IEEE Transactions on Pattern Analysis and Machine Intelligence, Vol. 20, Issue 12, pp. 1358-1364, 1998.
- [15] Papakostas, G.A., Boutalis, Y.S., Papaodysseues, C.N. and Fragoulis, D.K. "Numerical error analysis in Zernike Moments computation", Image and Vision Computing, Vol. 24, pp 960-969, 2009.